BULLETIN OF THE CHEMICAL SOCIETY OF JAPAN VOL. 43 789—793 (1970)

The Thermal Decomposition of Potassium Trioxalatoferrate(III) Trihydrate

Nobuyuki TANAKA and Katsuya SATO

Department of Chemistry, Faculty of Science, Tohoku University, Katahira-cho, Sendai

(Received August 29, 1969)

The thermal decomposition of $K_3[Fe(C_2O_4)_3]\cdot 3H_2O$ in solid state was studied by the thermogravimetric, the infrared spectroscopic and the manometric methods. It was found that, with elevating temperatures, three moles of water were evolved as the first step to form an anhydrous complex $K_3[Fe(C_2O_4)_3]$, which was then decomposed as the second step by an electron transfer from a ligand to the central iron(III) with the formation of an iron(II) complex. $K_2[Fe(C_2O_4)_2]$, $K_2C_2O_4$ and CO_2 were found as products in the second step. The total pressure of CO_2 gas evolved was measured at suitable time intervals. The shape of a curve of α (the fraction isothermally decomposed) *vs.* t (time) was sigmoidal. The initial part of the decomposition reaction was kinetically of a first-order and the activation energy was obtained to be 43.6 kcal/mol. A main part of it ($0.2<\alpha<0.8$) was of a second-order and obeyed the Prout-Tompkins' law. The activation energy was calculated to be 35.3 kcal/mol.

The thermal decomposition of anhydrous trioxalatoferrate(III) in solid state has been investigated by several researchers. From the polarographic and the infrared studies, Tanaka and Nanjo[1] reported that the thermal decomposition of this complex was initiated by an electron transfer from the coordinated oxalate ion to the central iron(III) forming iron(II) complex. From the thermogravimetric analysis (TGA) and the differential thermal analysis (DTA), Broadbent *et al.*[2] also indicated that a reduction of iron(III) to iron(II) takes place during the decomposition reaction. However, the stoichiometry of this reaction has not been fully determined and no kinetic studies have been reported. Therefore, it is worth while to determine the stoichiometry and to investigate the kinetics of this decomposition reaction. In this paper, the decomposition products which were identified by the thermogravimetric and the infrared spectroscopic methods and the kinetic parameters of this reaction which were obtained by the manometric method are presented. On the basis of the experimental results, possible reaction mechanisms are discussed.

Experimental

Materials. $K_3[Fe(C_2O_4)_3]\cdot 3H_2O$ was prepared with $FeCl_3\cdot 6H_2O$ and $K_2C_2O_4\cdot H_2O$. $K_2[Mn(C_2O_4)_2]$, $K_2[Co(C_2O_4)_2]$ and $K_2C_2O_4$ were prepared from their hydrates. $K_2[Mn(C_2O_4)_2]\cdot 2H_2O$ was prepared with $MnSO_4\cdot 4\sim 6H_2O$, $H_2C_2O_4\cdot 2H_2O$ and $K_2C_2O_4\cdot H_2O$. $K_2[Co(C_2O_4)_2]\cdot 6H_2O$ was prepared with $Co(NO_3)_2\cdot 6H_2O$, $H_2C_2O_4\cdot 2H_2O$ and $K_2C_2O_4\cdot H_2O$.

Apparatus and Procedure. The thermogravimetric curve was recorded with an automatic-recording thermobalance, Shimadzu Thermano Balance Type RT-2, in a nitrogen atmosphere. Two hundred milligrams of sample was used in each measurement. The furnace heating rate was about 4°C per min. The

1) N. Tanaka and M. Nanjo, This Bulletin, **40**, 330 (1967).

2) D. Broadbent, D. Dollimore and J. Dollimore, *J. Chem. Soc., A*, **1967**, 451.

particle size of the sample was smaller than 200 mesh.

A Hitachi EPI-2G double-beam infrared spectrophotometer equipped with a potassium bromide foreprism and gratings was used for the measurement of the infrared absorption spectra. The potassium bromide disk method was employed except the case of the identification of gaseous product.

The reflectance spectra were obtained on a Hitachi photo-electric spectrophotometer EPU-2 equipped with a standard reflectance attachment. Powdered magnesium oxide was used as a standard.

Decomposition pressure-time curves of the isothermal decomposition reaction were obtained by the manometric method. The temperature of the sample was controlled in a range of ± 0.5°C by means of a mercury regulator and an electric furnace. The measurement of isothermal decomposition of anhydrous trioxalato complex was carried out after hydrate sample was previously dehydrated at 120°C for 4 hr in each run. Samples which were smaller than 200 mesh in size weighed 33.5 mg in each run unless otherwise stated. The fraction decomposed in the pyrolysed sample, α, is calculated according to the equation,

$$\alpha = \frac{\text{Total } CO_2 \text{ pressure at time } t}{\text{Total } CO_2 \text{ pressure at the completion of reaction}}$$

The rate constants of the isothermal decomposition were obtained from the kinetic analysis of α-t curves. The kinetic parameters were calculated according to the Arrhenius equation.

Results and Discussion

Stoichiometric Studies. From the TGA curve of the trioxalatoferrate(III) as shown in Fig. 1, it

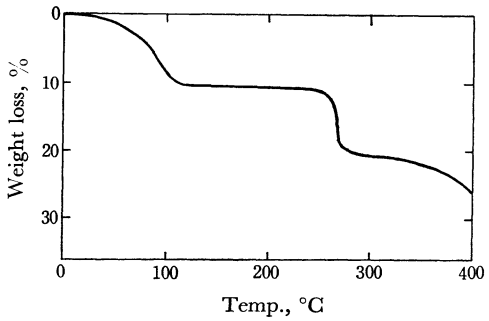

Fig. 1. Thermogravimetric curve of $K_3[Fe(C_2O_4)_3]\cdot 3H_2O$ obtained in nitrogen atmosphere.

can be seen that the first stage in the decomposition reaction begins at 30°C and completes at 120°C. The weight loss in this stage was determined to be 10.6%. This result agrees with the calculated weight loss of 11.00% for the loss of 3 mol of water. This dehydrated complex is thermally stable up to 230°C. The second stage in the decomposition reaction begins at 250°C and completes at 300°C. The weight loss was found to be 9.5% and the color change from green to yellow was observed. This weight loss is compared with the calculated value of 8.96% for the evolution of carbon dioxide, which was identified by the measurement of infrared spectra of the gaseous product.

In order to identify the solid-state decomposition products, infrared spectra were obtained with the samples which were completely decomposed and with some of other anhydrous complexes. They are shown in Fig. 2. The decomposition products

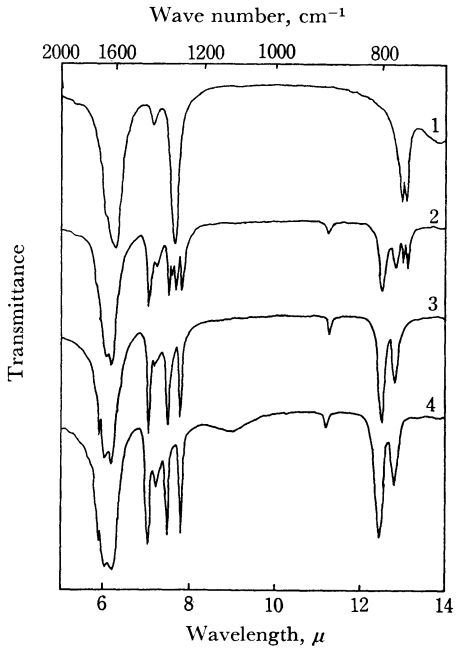

Fig. 2. Infrared absorption spectra of (1) $K_2C_2O_4$, (2) decomposition products, (3) $K_2[Mn(C_2O_4)_2]$ and (4) $K_2[Co(C_2O_4)_2]$. Transmittance scale is displaced arbitrarily.

give absorption bands at 764.5, 771.0 and 1305 cm^{-1} which are also observed with anhydrous potassium oxalate. This means that one component of the solid-state products is anhydrous potassium oxalate. The rests of the absorption bands of the products are similar to those of $K_2[Mn(C_2O_4)_2]$ and $K_2[Co(C_2O_4)_2]$. This indicates that another component of the products will be $K_2[Fe(C_2O_4)_2]$. The absorption band at 1289 cm^{-1} of the product, which was not observed with $K_2[Mn(C_2O_4)_2]$ and $K_2[Co(C_2O_4)_2]$, may be a characteristic one of $K_2[Fe(C_2O_4)_2]$. Unfortunately, however, the infrared absorption spectra of $K_2[Fe(C_2O_4)_2]$ could not be obtained because of the difficulty in the preparation of the complex. From the chemical analysis and the reflectance spectroscopic studies, Wendlandt and Simmons reported that decomposition products of the corresponding complexes of manganese(III)[3] and cobalt(III)[4] were also dioxalato complexes of

3) E. Simmons and W. Wendlandt, *J. Inorg. Nucl. Chem.*, **27**, 2325 (1965).

4) W. Wendlandt and E. Simmons, *ibid.*, **27**, 2317 (1965).

manganese(II) and cobalt(II), respectively. These facts support, though indirectly, the results obtained in this study.

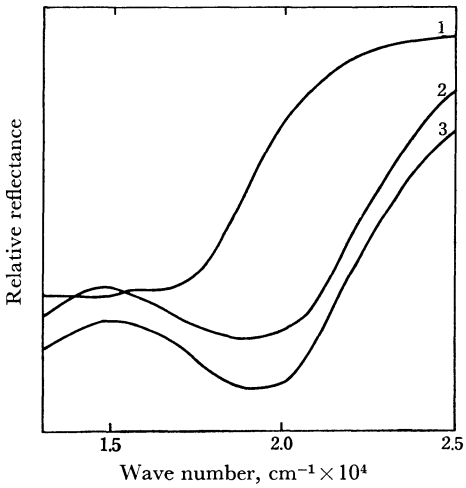

Fig. 3. Reflectance spectra of (1) decomposition products, (2) $K_3[Fe(C_2O_4)_3]$ and (3) $K_3[Fe(C_2O_4)_3]\cdot 3H_2O$. Relative reflectance scale is displaced arbitrarily.

The reflectance spectra of $K_3[Fe(C_2O_4)_3]\cdot 3H_2O$, $K_3[Fe(C_2O_4)_3]$ and its decomposition products are shown in Fig. 3. In the case of $K_3[Fe(C_2O_4)_3]\cdot 3H_2O$ and its anhydride, the absorption bands due to the d–d transition appear at 14925 cm^{-1} and 14706 cm^{-1}, respectively. Above 19000 cm^{-1}, the absorption of both compounds increases with increasing wave numbers. This means that the structure of $[Fe(C_2O_4)_3]^{3-}$ ion in $K_3[Fe(C_2O_4)_3]$ is similar to that in $K_3[Fe(C_2O_4)_3]\cdot 3H_2O$; the structure of $[Fe(C_2O_4)_3]^{3-}$ ion in the latter is octahedral. Of the decomposition products, which must be $K_2C_2O_4$ and $K_2[Fe(C_2O_4)_2]$, $K_2C_2O_4$ is transparent throughout all of the visible region of the spectrum, and therefore the absorption may be due to $K_2[Fe(C_2O_4)_2]$. It can be assumed that the structure of $[Fe(C_2O_4)_2]^{2-}$ ion is either tetrahedral or planar. If it is tetrahedral, only one absorption may appear, whereas if planar, several absorptions may appear because of a lower symmetry of crystal field. Actually, as $K_2[Fe(C_2O_4)_2]$ gives an absorption which increases gradually with increasing wave numbers as shown in Fig. 3 and its color is yellow, its structure may be tetrahedral. From all of these informations obtained in this study, the stoichiometry of the thermal decomposition reaction was estimated to be:

i) $K_3[Fe(C_2O_4)_3]\cdot 3H_2O \rightarrow K_3[Fe(C_2O_4)_3] + 3H_2O$

ii) $K_3[Fe(C_2O_4)_3] \rightarrow K_2[Fe(C_2O_4)_2] + \frac{1}{2}K_2C_2O_4 + CO_2$

In the case of photolysis,[5] the reduction product is a monooxalatoiron(II) complex. This means that the mechanism of the electron transfer to iron(III) is different from each other in the cases of the thermal and the photolytic decomposition.

Kinetic Studies. The kinetics of the decomposition reaction was investigated by the manometric measurements. A plot of α *vs.* t was sigmoidal when the anhydride was decomposed completely. It may be divided from the standpoint of kinetics into two stages; (a) the initial reaction which is fitted to a first-order rate law where α is smaller than 0.05, and (b) the main reaction which is fitted to the Prout-Tompkins' equation[6] where α is between 0.2 and 0.8.

(a) The Initial Reaction. At lower temperatures, the curves of α *vs.* t show the initial stage of the decomposition reaction. (See Fig. 4). The rate constant in this stage, k_1, was expressed by the equation,

$$\frac{d\alpha}{dt} = k_1(1-\alpha) \qquad (1)$$

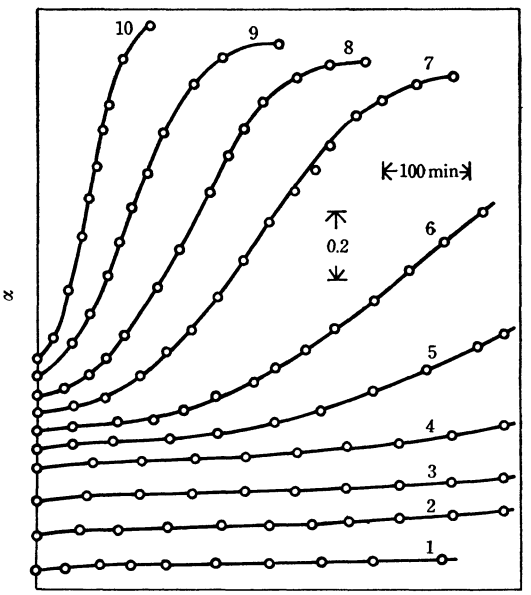

Fig. 4. Fractional decomposition as a function of time at (1) 180.5, (2) 183.2, (3) 184.0, (4) 186.5, (5) 190.5, (6) 195.3, (7) 201.0, (8) 205.0, (9) 210.5, and (10) 216.0°C.

Equation (1) is converted to

$$\ln(1-\alpha) = -k_1 t \qquad (2)$$

and the values of k_1 were determined from the slopes of $\log(1-\alpha)$ *vs.* t (Table 1). The Arrhenius plot for this stage is shown in Fig. 5. The kinetic equation derived from the Arrhenius plot is

5) W. Wendlandt and E. Simmons, *J. Inorg. Nucl. Chem.*, **28**, 2420 (1966).

6) E. Prout and F. Tompkins, *Trans. Faraday Soc.*, **40**, 488 (1944).

TABLE 1. RATE CONSTANTS FOR THE INITIAL REACTION (k_1) AND THE MAIN REACTION (k_2)

Temp. °C	$k_1 \times 10^6$ sec^{-1}	$k_2 \times 10^4$ sec^{-1}
180.5	1.03	—
183.2	1.27	—
184.0	1.60	—
186.5	2.00	—
190.5	3.02	1.10
195.3	4.76	1.52
201.0	8.27	2.38
205.0	—	3.40
210.5	—	4.58
216.0	—	8.51

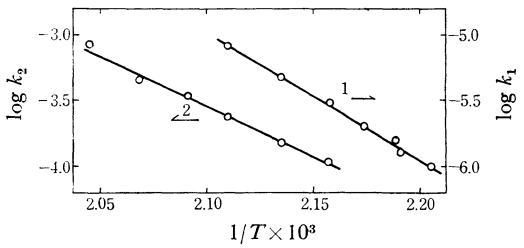

Fig. 5. Arrhenius plots for (1) the initial reaction (k_1) and (2) the main reaction (k_2).

$$\log k_1 = \frac{-43600}{2.3RT} + 14.9 \qquad (3)$$

(b) The Main Reaction. At higher temperatures, the experimental results were fitted to the Prout-Tompkins' equation,

$$\frac{d\alpha}{dt} = k_2(1-\alpha)\alpha \qquad (4)$$

over the range of $\alpha=0.2$ to 0.8. (See also Fig. 4). Equation (4) is converted to

$$\ln \frac{\alpha}{1-\alpha} = k_2 t \qquad (5)$$

The rate constant of the main reaction, k_2, was determined from the slope of $\log \alpha/(1-\alpha)$ *vs.* t (Table 1). The Arrhenius plot for this stage is also shown in Fig. 5. The activation parameters were determined as usual from the Arrhenius equation:

$$\log k_2 = \frac{-35300}{2.3RT} + 12.6 \qquad (6)$$

In the region where the rate obeyed to the Prout-Tompkins' law, the effects on the reaction rate were investigated under several experimental conditions. Changes in sample weight and particle size were found to give little difference in the rate constant as shown in Table 2; sample weight was changed from 10.0 to 33.5 mg and particle size, from 150~200 mesh to smaller than 200 mesh. The effect of pressure of carbon dioxide gas was also investigated. Pressure-time curves A, B and C measured are shown in Fig. 6. When curves B and C are shifted

TABLE 2. EFFECTS OF SAMPLE WEIGHT AND PARTICLE SIZE ON THE RATE CONSTANT k_2 FOR THE REACTION

Temp. °C	Sample weight* mg	Particle size mesh	$k_2 \times 10^4$ sec^{-1}
210.5	10.0	smaller than 200	4.69
210.5	15.1	smaller than 200	4.51
210.5	20.0	smaller than 200	4.57
210.5	33.5	smaller than 200	4.58
208.0	20.0	smaller than 200	3.92
208.0	20.0	150~200	3.96

* Weight is converted for hydrate.

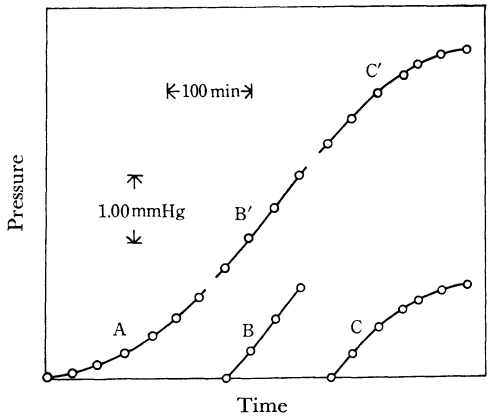

Fig. 6. Decomposition pressure of $K_3[Fe(C_2O_4)_3]$ as a function of time at 201.0°C, when system was evacuated at suitable time intervals (Curves A, B, and C). Curves B′ and C′ are obtained by shifting curves B and C in a proper way.

parallel to pressure axis, curves B′ and C′ are obtained. The shape of curve A-B′-C′ is identical with that obtained under the condition that the decomposition gas was not removed. This means that the rate of the decomposition reaction is not affected by the pressure of carbon dioxide gas. In order to investigate the reaction process, the mixture of $K_3[Fe(C_2O_4)_3]$ and its actual decomposition product and also the mixture of $K_3[Fe(C_2O_4)_3]$ and anhydrous $K_2C_2O_4$ were subjected to the thermal decomposition, because $K_2C_2O_4$ was considered to be one of the decomposition products. The rate constants obtained were compared with those ob-

TABLE 3. EFFECTS OF DECOMPOSITION PRODUCTS AND $K_2C_2O_4$ ON THE RATE CONSTANT k_2 FOR THE REACTION AT 208°C

Material added to $K_3[Fe(C_2O_4)_3]\cdot 3H_2O$ and its wieght percentage in parentheses	Total weight mg	$k_2 \times 10^4$ sec^{-1}
None	20	3.96
Actual decomposition product (16.7%)	25	3.83
$K_2C_2O_4\cdot H_2O$ (20%)	25	4.20

tained with $K_3[Fe(C_2O_4)_3]$ alone, when no significant difference was observed (Table 3). It was found that, as far as the main reaction is concerned, neither products nor potassium oxalate react chemically with $K_3[Fe(C_2O_4)_3]$, and they have no catalytic role in the decomposition reaction. It is said that chemical processes which give α *vs.* t plots of sigmoidal shape usually result from reactions which take place at the reactant-product interface.[7] This indicates that, when the decomposition products are mixed mechanically with the reactant before heating, the effective area of the reactant-product interface is much smaller than that which is actually produced in the course of reaction. The Prout-Tompkins' equation means the existence of the acceleration and the deceleration period. The former corresponds to the increase in the area of the reactant-product interface. In the latter, the reaction interface still continues to grow towards the central unreacted regions of the particle, but the interfacial area begins to overlap, and therefore the rate becomes deceleratory until the decomposition of the reactant is completed. Presumably, this reaction is controlled by the diffusion of the interface. Further evidence is necessary to state the relationship between the reaction mechanism and the Prout-Tompkins' law.

7) A. Galwey, "Chemistry of Solids," Chapman & Hall Ltd. (1967), Chapter 5.

The authors are grateful to Mr. Kenzo Nagase for advice and suggestion which he gave in the course of this study, and to Mr. Mitsuo Sato for the measurement of infrared absorption spectra. They also wish to thank the Ministry of Education for the financial support granted for this research.